Editors' Suggestion | Featured in Physics

# Network Effects Lead to Self-Organization in Metabolic Cycles of Self-Repelling Catalysts

Vincent Ouazan-Reboul,[1] Ramin Golestanian,[1,2,*] and Jaime Agudo-Canalejo[1,†]
[1]Max Planck Institute for Dynamics and Self-Organization, Am Fassberg 17, D-37077 Göttingen, Germany
[2]Rudolf Peierls Centre for Theoretical Physics, University of Oxford, Oxford OX1 3PU, United Kingdom

(Received 18 April 2023; accepted 27 July 2023; published 19 September 2023)

Mixtures of particles that interact through phoretic effects are known to aggregate if they belong to species that exhibit attractive self-interactions. We study self-organization in a model metabolic cycle composed of three species of catalytically active particles that are chemotactic toward the chemicals that define their connectivity network. We find that the self-organization can be controlled by the network properties, as exemplified by a case where a collapse instability is achieved by design for self-repelling species. Our findings highlight a possibility for controlling the intricate functions of metabolic networks by taking advantage of the physics of phoretic active matter.

DOI: 10.1103/PhysRevLett.131.128301

*Introduction.*—Catalyzed chemical reactions are intrinsically and locally out of equilibrium, making catalytic particles a paradigmatic example of systems in which the physics of active matter comes into play [1]. In particular, catalytic activity coupled to a chemotactic, gradient-response mechanism such as diffusiophoresis [2,3] enables the self-propulsion of individual colloidal particles via self-phoresis [4,5], as well as collective behavior mediated by effective interactions between active colloids [6–10]. In addition, catalytic activity is essential to the function of biological systems, allowing for the occurrence, as a part of metabolism, of reactions that would otherwise be kinetically inhibited [11]. Metabolic processes often require enzymatic catalysis to occur in a space- and time-localized manner, necessitating some degree of self-organization of the participating enzymes [12–19]. In particular, many enzymes have been shown to spontaneously form transient aggregates, known as metabolons [20].

Simple cases of spontaneous self-organization in mixtures of several catalytic components have been previously studied both in theory [21–26] and in experiment [27–31]. However, the influence of the sometimes complex topology of reaction networks on the self-organization of the metabolic components has not yet been elucidated. Indeed, many catalytic processes of biological and industrial significance —from cellular metabolism [32] to carbon fixation [33]— involve a closed chain of catalytic reactions, where the product of one catalyst is passed on as the substrate of the next one, i.e., a metabolic cycle. Because the spatial arrangement of catalysts may strongly affect the overall rate of the reactions [17,18,26], it is important to understand under which conditions such spatial reorganization may happen spontaneously and whether it can be triggered in generically stable systems via network-mediated effects. In this Letter, we study the chemotactic self-organization of three species of catalytically active particles that participate in a model catalytic cycle. We find that a mixture of only self-repelling catalytic species can undergo self-organization via network effects emerging from the metabolic cycle topology.

*Model.*—We consider catalytically active particles that produce and consume a set of chemicals, with activities $\alpha_m^{(k)}$ corresponding to the rate of production (if positive) or consumption (if negative) of chemical $k$ by active species $m$. These particles are also chemotactic: synthetic colloids typically move via hydrodynamic-phoretic mechanisms [1,27,28,31]; whereas the mechanism underlying the observed chemotaxis of biological enzymes is still debated [34–42]. In a concentration gradient of chemical $k$, species $m$ develops a velocity $\mathbf{v}_m^{(k)} = -\mu_m^{(k)}\boldsymbol{\nabla} c^{(k)}$, where $\mu_m^{(k)}$ is a mobility coefficient. The combination of catalytic and chemotactic activities results in effective interactions between the active species going as $\mathbf{v}_{m,n} \propto \sum_k \alpha_n^{(k)}\mu_m^{(k)}$, where $\mathbf{v}_{m,n}$ represents the velocity of $m$ in response to the presence of $n$; see Fig. 1(a). Importantly, these interactions are nonreciprocal, in the sense that we generically have $\mathbf{v}_{m,n} \neq -\mathbf{v}_{n,m}$ [21].

We use a continuum model for the concentration $\rho_m$ of the active species $m$ and the chemical concentration $c^{(k)}$, which reads

$$\partial_t \rho_m(\mathbf{r},t) = \boldsymbol{\nabla}\cdot\left[D_p\boldsymbol{\nabla}\rho_m + \sum_k \mu_m^{(k)}(\boldsymbol{\nabla}c^{(k)})\rho_m\right], \quad (1a)$$

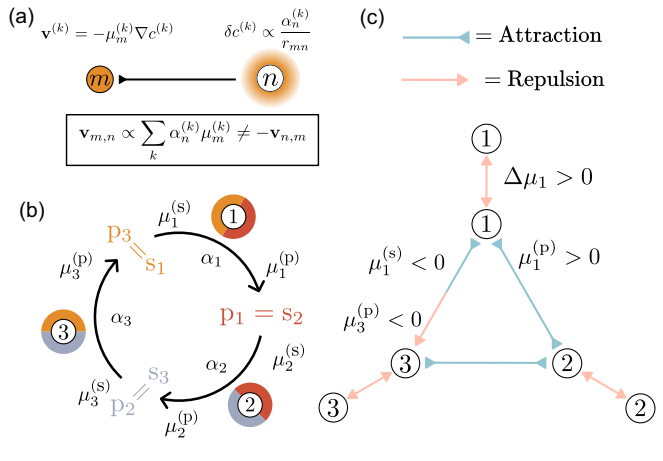


FIG. 1. (a) Emergence of field-mediated, nonreciprocal interactions between particle $n$, which perturbs the chemical field $c^{(k)}$ around itself, and particle $m$, which develops a velocity in response to the resulting chemical gradient. (b) Metabolic cycle of three species. Each converts their substrate into a product that acts as the substrate of the next species and moves in response to gradients of both chemicals. (c) Example of a set of species-species interactions emerging from the combination of effective field-mediated interactions and metabolic cycle topology. With this particular choice of parameters, each species is self-repelling, and the species pair 1–3 exhibits chasing interactions.

$$\partial_t c^{(k)}(\mathbf{r},t) = D^{(k)}\boldsymbol{\nabla}^2 c^{(k)} + \sum_m \alpha_m^{(k)}\rho_m. \tag{1b}$$

Here, Eq. (1) is a continuity equation with $D_p$ being the diffusion coefficient of the colloidal particles, which we assumed to be equal for all active particles for simplicity, and the drift velocity following the concentration gradients of all chemicals. Moreover, Eq. (1b) is a reaction-diffusion equation for the chemicals, with $D^{(k)}$ representing the diffusion coefficient of chemical $(k)$, and the reaction term accounting for the local activity of all catalytic species.

To determine when such a mixture undergoes an instability, we perform a linear stability analysis of these equations [43]. We find that a perturbation $(\delta\rho_m, \delta c^{(k)})$ around an initially homogeneous state $(\rho_{0m}, c_h^{(k)})$ follows the general eigenvalue equation $-\sum_{n=1}^{M}\Lambda_{m,n}\delta\rho_n = [\lambda + D_p q^2]\delta\rho_m$, where $\Lambda_{m,n} = \sum_k [\alpha_n^{(k)}\mu_m^{(k)}/D^{(k)}]\rho_{0m}$ represents the response of species $m$ to species $n$, mediated by all chemical fields, and $\lambda(q)$ is the growth rate of a perturbation with wave number $q$. The coefficient $\Lambda_{m,n}$ is negative (positive) if species $m$ is attracted to (repelled by) species $n$. Throughout the rest of this Letter, we rescale the mobility coefficients for brevity, such that $\mu_m^{(k)}/D^{(k)} \to \mu_m^{(k)}$. The system undergoes an instability if any mode has a positive growth rate $\lambda > 0$. We focus on the eigenvalue with the highest growth rate associated with the $q^2 = 0$ mode, corresponding to the longest wavelength, which represents a macroscopic instability.

*Metabolic cycles.*—We focus on the particular case of metabolic cycles composed of three active species [Fig. 1(b)], where species $m$ converts its substrate $s_m$ into its product $p_m = s_{m+1}$, with catalytic activity $\alpha_m = \alpha_m^{(p_m)} = -\alpha_m^{(s_m)} > 0$, as depicted in Fig. 1(b). As the cycle is closed, the species indices are periodic, with species 4 being identical to species 1, and species 0 being identical to species 3.

The species have a chemotactic response to both their substrate and product, with respective mobilities $\mu_m^{(s)} \equiv \mu_m^{(m)}$ and $\mu_m^{(p)} \equiv \mu_m^{(m+1)}$. The resulting interaction matrix has the following (nonvanishing) coefficients [Fig. 1(c)]: $\Lambda_{m,m-1} = \alpha_{m-1}\mu_m^{(s)}\rho_{0m}$, $\Lambda_{m,m} = \alpha_m\Delta\mu_m\rho_{0m}$, and $\Lambda_{m,m+1} = -\alpha_{m+1}\mu_m^{(p)}\rho_{0m}$, where $\Delta\mu_m \equiv \mu_m^{(p)} - \mu_m^{(s)}$ and is, in general, asymmetric, reflecting the nonreciprocal nature of the interactions between the catalytic species.

We now calculate the eigenvalues $\lambda(q=0)$ for $\Lambda_{m,n}$ as defined above and find two eigenvalues given by [43]

$$\lambda_\pm = -\frac{1}{2}\sum_{m=1}^{3}\alpha_m\Delta\mu_m\rho_{0m} \pm \frac{1}{2}\sqrt{\left(\sum_{m=1}^{3}\alpha_m\Delta\mu_m\rho_{0m}\right)^2 - 4\sum_{m=1}^{3}\alpha_m\alpha_{m+1}\left(\Delta\mu_m\Delta\mu_{m+1} + \mu_m^{(p)}\mu_{m+1}^{(s)}\right)\rho_{0m}\rho_{0m+1}}, \tag{2}$$

as well as one null eigenvalue $\lambda_0 = 0$. The system will be linearly unstable when (the real part of) the largest eigenvalue $\lambda_+$ becomes positive.

*Substrate-sensitive species.*—A simple class of cycles whose parameter space can be explored in full generality involves those in which the catalytic particles are only chemotactic toward their substrate, i.e., $\mu_m^{(p)} = 0$. This subset of cycles is particularly relevant, as most experiments on enzymes have shown them to chemotax in concentration gradients of their substrate [35,37,38].

We thus have three activities $\alpha_m$ and three substrate mobilities $\mu_m^{(s)}$, with the mobility difference reducing to $\Delta\mu_m = -\mu_m^{(s)}$. Species in such a cycle then only interact with the previous species in the cycle and with themselves, with $\Lambda_{m,m-1} = \alpha_{m-1}\mu_m^{(s)}\rho_{0m}$, $\Lambda_{m,m} = -\alpha_m\mu_m^{(s)}\rho_{0m}$, and $\Lambda_{m,m+1} = 0$. Note that the self-interaction always has the opposite sign to the interaction with the previous species in the cycle, which further limits the possible interaction patterns the catalytic species can exhibit.

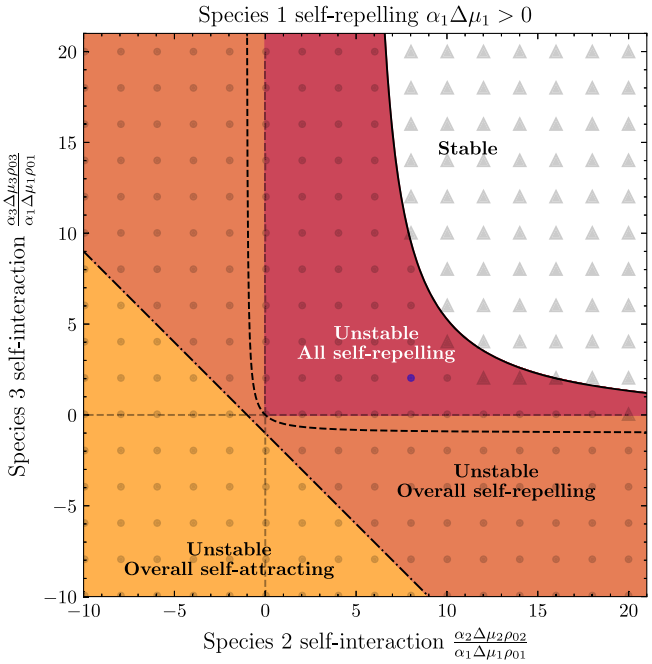


FIG. 2. Stability phase diagram for cycles involving at least one self-repelling species. Species 1 taken to be self-repelling ($\alpha_1\Delta\mu_1 > 0$). Solid line: stability line in normalized self-interaction plane for a specific choice of parameters. Dashed line: parameter-free instability line below which cycles with null product mobilities $\mu^{(p)}_{1,2,3} = 0$ are unstable. Note that this line lies always below the top-right, all-self-repelling quadrant. Dash-dotted line: parameter-free boundary between overall self-attracting and self-repelling catalytic mixtures. Gray markers: coordinates of Brownian dynamics simulations, found to be unstable if the marker is a circle or stable if it is a triangle. The blue marker corresponds to the coordinates of the simulation shown in Fig. 3. For the expressions of the stability lines and the values of the parameters, see the Supplemental Material [43].

In the context of this reduced parameter space, and assuming species 1 is self-repelling (i.e. $\alpha_1\Delta\mu_1 > 0$), one can solve $\mathrm{Re}(\lambda_+) > 0$ for all parameter values, yielding a comprehensive two-dimensional stability phase diagram as shown in Fig. 2 [43], which depends only the normalized self-interactions $(\alpha_2\Delta\mu_2\rho_{02}/\alpha_1\Delta\mu_1\rho_{01})$ and $(\alpha_3\Delta\mu_3\rho_{03}/\alpha_1\Delta\mu_1\rho_{01})$. The corresponding parameter-free instability line is plotted as a dashed line on Fig. 2, with the dark orange and light orange regions below that line corresponding to unstable metabolic cycles. As the instability line is above the light orange region corresponding to overall self-attracting mixtures in Fig. 2 ($\sum_{m=1}^{3}\Lambda_{m,m} < 0$), we uncover that it is not necessary for the metabolic cycle to be composed of overall self-attracting species in order to self-organize, as opposed to mixtures involving simpler interaction schemes [22,25,46] or metabolic cycles of two species [43]. This result does not, however, extend to cycles composed only of self-repelling species ($\Lambda_{m,m} > 0$ for all $m$), which are always stable, as shown by the fact that the corresponding top-right quadrant in Fig. 2 is always above the dashed stability line. This implies that some amount of self-attraction is still necessary for the catalytic particles to self-organize in this limited interaction network.

*Self-organization of purely self-repelling species.*—We now consider the general case with both nonzero substrate and product mobilities, for which each species interacts with both the previous and the next species in the cycle according to a pattern set by its substrate mobility $\mu^{(s)}$, its product mobility $\mu^{(p)}$, and their difference $\Delta\mu$. By solving for $\mathrm{Re}(\lambda_+) > 0$ in Eq. (2), we find that a cycle that is overall self-repelling can be made unstable provided the following condition is satisfied:

$$\sum_{m=1}^{3}\alpha_m\Delta\mu_m\rho_{0m}\,\alpha_{m+1}\Delta\mu_{m+1}\rho_{0m+1} < -\sum_{m=1}^{3}\alpha_m\mu^{(s)}_{m+1}\rho_{0m+1}\,\alpha_{m+1}\mu^{(p)}_{m}\rho_{0m}. \tag{3}$$

The condition (3), which involves terms mixing pairs of catalytic species, can be rewritten as $\sum\Lambda_{m,m}\Lambda_{m+1,m+1} < \sum\Lambda_{m,m+1}\Lambda_{m+1,m}$ and thus sets a bound on the self-interactions of pairs of species relative to their cross-interactions. This inequality implies that, in the case of an overall self-repelling cycle where $\sum_{m=1}^{3}\Lambda_{m,m} > 0$, the presence of species pairs that interact reciprocally offer an alternate route to instability.

We find that a striking new feature of this general case is that cycles composed only of self-repelling species ($\Delta\mu_m > 0$ for all $m$) can be unstable. More specifically, if any of the species $m$ verifies one of the following inequalities [43]:

$$\alpha_{m+1}\mu^{(p)}_{m+1}\rho_{0m+1} > \alpha_m\Delta\mu_m\rho_{0m}, \tag{4a}$$

$$\mu^{(s)}_{m} > 0, \tag{4b}$$

$$\frac{1}{\alpha_m\mu^{(s)}_m\rho_{0m}}\Big[\alpha_{m-1}\mu^{(p)}_{m-1}\rho_{0m-1}\alpha_m\mu^{(s)}_m\rho_{0m} + \alpha_{m+1}\mu^{(p)}_{m+1}\rho_{0m+1}\Big(\alpha_m\mu^{(p)}_m\rho_{0m} + \alpha_{m-1}\mu^{(p)}_{m-1}\rho_{0m-1}\Big)\Big] > 0, \tag{4c}$$

a region of the parameter space exists (in red in Fig. 2) in which a set of three self-repelling species is unstable according to the condition given in Eq. (3). This behavior is illustrated, for a particular set of parameters for which species 1 obeys inequalities Eqs. (4a) and (4c), by the stability phase diagram shown in Fig. 2. For this choice of parameters, the stability line is contained in the top-right quadrant, which corresponds to a mixture of three self-repelling species. Thus, in some regions of the parameter space (Fig. 2, dark red), the destabilizing pair interactions

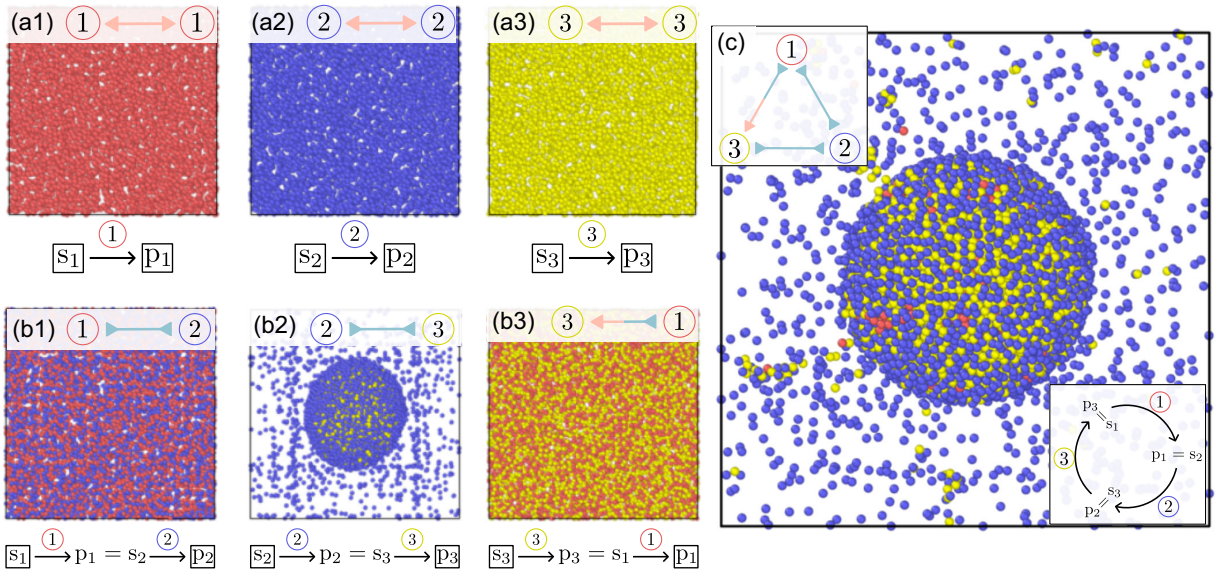


FIG. 3. Instability of a generic three-enzyme cycle triggered by the presence of a single instability-favoring pair. (a1)–(a3) Single-species interactions: all particle species are self-repelling, and thus single-species suspensions stay homogeneous. (b1)–(b3) Pair interactions: of the two-species mixtures, 1-2 and 3-1 mixtures form small molecules but remain homogeneous, while 2-3 is unstable and results in the formation of a 2-3 cluster coexisting with a gas of species 2. (c) Despite all species being self-repelling, the instability of the 2-3 pair causes the instability of the full three-species mixture, resulting in the formation of a cluster, which coexists with a gas of species 2. Note that species 1 (red) also participates in the cluster, despite not aggregating with either of the other species (b1),(b3). In all panels, the inset at the top represents the effective interactions among species, whereas the corresponding chemical reaction network is depicted at the bottom. The reaction networks in (a),(b) are *open*, as they involve substrates and products that must be externally supplied or removed (boxed $s_m$ and $p_m$). The full reaction network in (c) is *closed*. See also the Supplemental Material and Videos 1–7 in [43] for a description of the simulation parameters and videos.

are able to overcome self-repulsion and lead to the formation of a cluster of three species in the absence of self-attraction. We recall that cycles of strictly substrate-sensitive species, which are stable above the dashed line drawn in Fig. 2, exhibit no such region independent of the choice of parameters. An increased complexity of interactions is therefore needed in order to overcome self-repulsion. Note in particular that, while condition (4b) appears simple, repulsion from the substrate ($\mu_m^{(s)} > 0$) acts against self-repulsion ($\Delta\mu_m > 0$). Requiring both conditions simultaneously implies that $\mu_m^{(p)} > \mu_m^{(p)} > 0$, i.e., species $m$ must be repelled from its product particularly strongly (more than it is repelled from its substrate). We have confirmed this analytical prediction using Brownian dynamics simulations (Fig. 2, gray circles and triangles). By scanning the coordinates of Fig. 2 for a set of parameters given in the Supplemental Material [43], we broadly recover the predicted instability line.

The results of a simulation of an unstable cycle of three self-repelling species, with parameters corresponding to the blue point in Fig. 2 and the interactions shown in Fig. 1(c), are shown in Fig. 3 (see Ref. [43] for simulation parameters). In order to uncover the (de)stabilizing effect of each species or species pair, we simulate solutions of one (a) and two (b) species that interact in the same manner as they would in the full cycle. In Figs. 3(a1)–3(a3), we find that each catalytic species taken on its own does not cluster, because of being self-repelling. Figures 3(b1) and 3(b3) demonstrate that mixtures of particles belonging to species pairs (1,2) and (3,1), when considered together, are also stable and lead to the formation of small dynamic molecules. However, as shown in Fig. 3(b2), mixtures of particles of species 2 and 3 are unstable and lead to the formation of a mixed cluster coexisting with a dilute phase. A favorable choice of parameters allows species 2 and 3 to destabilize the whole ternary (1,2,3) mixture of catalysts, despite the stabilizing effects of the individual species and the rest of the species pairs. The resulting structure is a cluster mixing all three species coexisting with a dilute phase.

*Discussion.*—Using a simple model, we have shown that three catalytically active species involved in a model metabolic cycle are able to undergo a self-organizing instability through chemical field-mediated effective interactions. In the case of a cycle involving species that are only chemotactic toward their substrates, we find that, while self-organization is possible if the mixture of catalytic species is overall self-repelling, at least one of the species must be self-attracting for the instability to occur. However, in contrast to this case and to what was previously known for phoretic particles [22,25,46], we find

that the system can self-organize even when all species are self-repulsive through instability-favoring pair interactions, in the general case of species chemotactic to both their substrates and products. Clustering of self-repelling particle species is an already known phenomenon in active matter, for instance, driven by a mixture of short-range repulsion and self-propulsion [47,48]. The system we described here constitutes a new example of this phenomenon with unique features, exhibiting clustering through long-ranged interactions tied to complex reaction networks.

We found here that the topology of the reaction network between catalytically active particles can tightly couple to the spatial self-organization phenomena that they display. While we considered minimal catalytic cycles with only three species, future work may explore larger, biologically realistic cycles. Interestingly, our Letter shows that, for a three-species cycle, instability can occur if the species are overall self-attracting or if a more complex condition involving pairs of species [Eq. (3)] is satisfied. We speculate that, for larger cycles, additional higher-order conditions involving groups of three and more species may exist, further facilitating self-organization in these systems. Numerical experiments with randomly generated cycles seem to confirm this expectation [43]. In related work, we have also shown that the number of species in the cycle can have a strong effect on the resulting dynamics, with cycles of even and odd number of species displaying entirely different behavior [46]. Future work may also consider noncyclic topologies of the catalytic network (e.g., branched), as well as the effect of self-organization on the metabolic properties of the system [15,17–19,26]. Furthermore, our work may find application in engineering synthetic functional structures with shape-shifting capacity at the microscopic or molecular scale [49]. In particular, experiments exploring metabolism-induced self-organization could be performed using mixtures of colloids coated with different enzymes that participate in the same catalytic pathway [50,51].

This work has received support from the Max Planck School Matter to Life and the MaxSynBio Consortium, which are jointly funded by the Federal Ministry of Education and Research (BMBF) of Germany, and the Max Planck Society.

*ramin.golestanian@ds.mpg.de
†jaime.agudo@ds.mpg.de

[1] R. Golestanian, Phoretic active matter, in *Active Matter and Nonequilibrium Statistical Physics: Lecture Notes of the Les Houches Summer School: Volume 112, September 2018* (Oxford University Press, New York, 2022).
[2] J. Anderson, Colloid transport by interfacial forces, Annu. Rev. Fluid Mech. **21**, 61 (1989).
[3] F. Jülicher and J. Prost, Generic theory of colloidal transport, Eur. Phys. J. E **29**, 27 (2009).
[4] W. F. Paxton, K. C. Kistler, C. C. Olmeda, A. Sen, S. K. St. Angelo, Y. Cao, T. E. Mallouk, P. E. Lammert, and V. H. Crespi, Catalytic nanomotors: Autonomous movement of striped nanorods, J. Am. Chem. Soc. **126**, 13424 (2004).
[5] R. Golestanian, T. B. Liverpool, and A. Ajdari, Designing phoretic micro- and nano-swimmers, New J. Phys. **9**, 126 (2007).
[6] I. Theurkauff, C. Cottin-Bizonne, J. Palacci, C. Ybert, and L. Bocquet, Dynamic Clustering in Active Colloidal Suspensions with Chemical Signaling, Phys. Rev. Lett. **108**, 268303 (2012).
[7] I. Buttinoni, J. Bialké, F. Kümmel, H. Löwen, C. Bechinger, and T. Speck, Dynamical Clustering and Phase Separation in Suspensions of Self-Propelled Colloidal Particles, Phys. Rev. Lett. **110**, 238301 (2013).
[8] S. Saha, R. Golestanian, and S. Ramaswamy, Clusters, asters, and collective oscillations in chemotactic colloids, Phys. Rev. E **89**, 062316 (2014).
[9] O. Pohl and H. Stark, Dynamic Clustering and Chemotactic Collapse of Self-Phoretic Active Particles, Phys. Rev. Lett. **112**, 238303 (2014).
[10] B. Liebchen, D. Marenduzzo, and M. E. Cates, Phoretic Interactions Generically Induce Dynamic Clusters and Wave Patterns in Active Colloids, Phys. Rev. Lett. **118**, 268001 (2017).
[11] R. Phillips, J. Kondev, J. Theriot, H. G. Garcia, and N. Orme, *Physical Biology of the Cell*, 2nd ed. (Garland Science, New York, 2012).
[12] C. A. Kerfeld, C. Aussignargues, J. Zarzycki, F. Cai, and M. Sutter, Bacterial microcompartments, Nat. Rev. Microbiol. **16**, 277 (2018).
[13] J.-L. Liu, The cytoophidium and its kind: Filamentation and compartmentation of metabolic enzymes, Annu. Rev. Cell Dev. Biol. **32**, 349 (2016).
[14] T. Selwood and E. K. Jaffe, Dynamic dissociating homo-oligomers and the control of protein function, Arch. Biochem. Biophys. **519**, 131 (2012).
[15] J. E. Dueber, G. C. Wu, G. R. Malmirchegini, T. S. Moon, C. J. Petzold, A. V. Ullal, K. L. Prather, and J. D. Keasling, Synthetic protein scaffolds provide modular control over metabolic flux, Nat. Biotechnol. **27**, 753 (2009).
[16] S. Kufer, E. Puchner, H. Gumpp, T. Liedl, and H. Gaub, Single-molecule cut-and-paste surface assembly, Science **319**, 594 (2008).
[17] F. Hinzpeter, F. Tostevin, and U. Gerland, Regulation of reaction fluxes via enzyme sequestration and co-clustering, J. R. Soc. Interface **16**, 20190444 (2019).
[18] F. Hinzpeter, F. Tostevin, A. Buchner, and U. Gerland, Trade-offs and design principles in the spatial organization of catalytic particles, Nat. Phys. **18**, 203 (2022).
[19] Y. Xiong, S. Tsitkov, H. Hess, O. Gang, and Y. Zhang, Microscale colocalization of cascade enzymes yields activity enhancement, ACS Nano **16**, 10383 (2022).
[20] L. J. Sweetlove and A. R. Fernie, The role of dynamic enzyme assemblies and substrate channelling in metabolic regulation, Nat. Commun. **9**, 2136 (2018).
[21] R. Soto and R. Golestanian, Self-Assembly of Catalytically Active Colloidal Molecules: Tailoring Activity through Surface Chemistry, Phys. Rev. Lett. **112**, 068301 (2014).

[22] J. Agudo-Canalejo and R. Golestanian, Active Phase Separation in Mixtures of Chemically Interacting Particles, Phys. Rev. Lett. **123**, 018101 (2019).
[23] J. Grauer, H. Löwen, A. Be'er, and B. Liebchen, Swarm hunting and cluster ejections in chemically communicating active mixtures, Sci. Rep. **10**, 5594 (2020).
[24] G. Giunta, H. Seyed-Allaei, and U. Gerland, Cross-diffusion induced patterns for a single-step enzymatic reaction, Commun. Phys. **3**, 167 (2020).
[25] V. Ouazan-Reboul, J. Agudo-Canalejo, and R. Golestanian, Non-equilibrium phase separation in mixtures of catalytically active particles: Size dispersity and screening effects, Eur. Phys. J. E **44**, 113 (2021).
[26] M. W. Cotton, R. Golestanian, and J. Agudo-Canalejo, Catalysis-Induced Phase Separation and Autoregulation of Enzymatic Activity, Phys. Rev. Lett. **129**, 158101 (2022).
[27] T. Yu, P. Chuphal, S. Thakur, S. Y. Reigh, D. P. Singh, and P. Fischer, Chemical micromotors self-assemble and self-propel by spontaneous symmetry breaking, Chem. Commun. **54**, 11933 (2018).
[28] F. Schmidt, B. Liebchen, H. Löwen, and G. Volpe, Light-controlled assembly of active colloidal molecules, J. Chem. Phys. **150**, 094905 (2019).
[29] C. H. Meredith, P. G. Moerman, J. Groenewold, Y.-J. Chiu, W. K. Kegel, A. van Blaaderen, and L. D. Zarzar, Predator–prey interactions between droplets driven by non-reciprocal oil exchange, Nat. Chem. **12**, 1136 (2020).
[30] A. Testa, M. Dindo, A. A. Rebane, B. Nasouri, R. W. Style, R. Golestanian, E. R. Dufresne, and P. Laurino, Sustained enzymatic activity and flow in crowded protein droplets, Nat. Commun. **12**, 6293 (2021).
[31] J. Grauer, F. Schmidt, J. Pineda, B. Midtvedt, H. Löwen, G. Volpe, and B. Liebchen, Active droploids, Nat. Commun. **12**, 6005 (2021).
[32] F. Wu, L. N. Pelster, and S. D. Minteer, Krebs cycle metabolon formation: Metabolite concentration gradient enhanced compartmentation of sequential enzymes, Chem. Commun. **51**, 1244 (2015).
[33] T. Schwander, L. Schada von Borzyskowski, S. Burgener, N. S. Cortina, and T. J. Erb, A synthetic pathway for the fixation of carbon dioxide *in vitro*, Science **354**, 900 (2016).
[34] H. Yu, K. Jo, K. L. Kounovsky, J. J. de Pablo, and D. C. Schwartz, Molecular propulsion: Chemical sensing and chemotaxis of DNA driven by RNA polymerase, J. Am. Chem. Soc. **131**, 5722 (2009).
[35] S. Sengupta, K. K. Dey, H. S. Muddana, T. Tabouillot, M. E. Ibele, P. J. Butler, and A. Sen, Enzyme molecules as nanomotors, J. Am. Chem. Soc. **135**, 1406 (2013).
[36] K. K. Dey, S. Das, M. F. Poyton, S. Sengupta, P. J. Butler, P. S. Cremer, and A. Sen, Chemotactic separation of enzymes, ACS Nano **8**, 11941 (2014).
[37] X. Zhao, H. Palacci, V. Yadav, M. M. Spiering, M. K. Gilson, P. J. Butler, H. Hess, S. J. Benkovic, and A. Sen, Substrate-driven chemotactic assembly in an enzyme cascade, Nat. Chem. **10**, 311 (2018).
[38] A.-Y. Jee, Y.-K. Cho, S. Granick, and T. Tlusty, Catalytic enzymes are active matter, Proc. Natl. Acad. Sci. U.S.A. **115**, E10812 (2018).
[39] J. Agudo-Canalejo, T. Adeleke-Larodo, P. Illien, and R. Golestanian, Enhanced diffusion and chemotaxis at the nanoscale, Acc. Chem. Res. **51**, 2365 (2018).
[40] J. Agudo-Canalejo, P. Illien, and R. Golestanian, Phoresis and Enhanced diffusion compete in enzyme chemotaxis, Nano Lett. **18**, 2711 (2018).
[41] J. Agudo-Canalejo and R. Golestanian, Diffusion and steady state distributions of flexible chemotactic enzymes, Eur. Phys. J. Special Topics **229**, 2791 (2020).
[42] M. Feng and M. K. Gilson, Enhanced diffusion and chemotaxis of enzymes, Annu. Rev. Biophys. **49**, 87 (2020).
[43] See Supplemental Material at http://link.aps.org/supplemental/10.1103/PhysRevLett.131.128301 for details on the linear stability analysis, the case of two-species cycles, numerical results on cycles with more than three species, and the Brownian dynamics simulations, including Refs. [44,45].
[44] P. Strating, Brownian dynamics simulation of a hard-sphere suspension, Phys. Rev. E **59**, 2175 (1999).
[45] M. P. Allen and D. J. Tildesley, *Computer Simulation of Liquids* (Oxford University Press, New York, 2017).
[46] V. Ouazan-Reboul, J. Agudo-Canalejo, and R. Golestanian, Self-organization of primitive metabolic cycles due to non-reciprocal interactions, Nat. Commun. **14**, 4496 (2023).
[47] Y. Fily and M. C. Marchetti, Athermal Phase Separation of Self-Propelled Particles with No Alignment, Phys. Rev. Lett. **108**, 235702 (2012).
[48] M. E. Cates and J. Tailleur, Motility-induced phase separation, Annu. Rev. Condens. Matter Phys. **6**, 219 (2015).
[49] S. Osat and R. Golestanian, Non-reciprocal multifarious self-organization, Nat. Nanotechnol. **18**, 79 (2022).
[50] K. K. Dey, X. Zhao, B. M. Tansi, W. J. Méndez-Ortiz, U. M. Córdova-Figueroa, R. Golestanian, and A. Sen, Micromotors powered by enzyme catalysis, Nano Lett. **15**, 8311 (2015).
[51] X. Ma, A. C. Hortelão, T. Patino, and S. Sanchez, Enzyme catalysis to power micro/nanomachines, ACS Nano **10**, 9111 (2016).